Psychological Medicine

cambridge.org/psm

Neuroimaging and epigenetic analysis reveal novel epigenetic loci in major depressive disorder

Hyun-Ho Yang[1,*], Kyu-Man Han[2,3,*], Aram Kim[4], Youbin Kang[4], Woo-Suk Tae[3], Mi-Ryung Han[1] and Byung-Joo Ham[2,3]

[1]Division of Life Sciences, College of Life Sciences and Bioengineering, Incheon National University, Incheon, Republic of Korea; [2]Department of Psychiatry, Korea University Anam Hospital, Korea University College of Medicine, Seoul, Republic of Korea; [3]Brain Convergence Research Center, Korea University College of Medicine, Seoul, Republic of Korea and [4]Department of Biomedical Sciences, Korea University College of Medicine, Seoul, Republic of Korea

Original Article

*The first two authors have contributed equally to this article as co-first authors.

Cite this article: Yang H-H, Han K-M, Kim A, Kang Y, Tae W-S, Han M-R, Ham B-J (2024). Neuroimaging and epigenetic analysis reveal novel epigenetic loci in major depressive disorder. *Psychological Medicine* **54**, 2585–2598. https://doi.org/10.1017/S0033291724000709

Received: 15 June 2023
Revised: 20 February 2024
Accepted: 26 February 2024
First published online: 9 May 2024

Keywords:
cortical thickness; EWAS; major depressive disorder; neuroimaging-epigenetic study

Corresponding author:
Mi-Ryung Han;
Email: genetic0309@inu.ac.kr;
Byung-Joo Ham;
Email: hambj@korea.ac.kr

Abstract

Background. Epigenetic modifications, such as DNA methylation, contribute to the pathophysiology of major depressive disorder (MDD). This study aimed to identify novel MDD-associated epigenetic loci using DNA methylation profiles and explore the correlations between epigenetic loci and cortical thickness changes in patients with MDD.

Methods. A total of 350 patients with MDD and 161 healthy controls (HCs) were included in the epigenome-wide association studies (EWAS). We analyzed methylation, copy number alteration (CNA), and gene network profiles in the MDD group. A total of 234 patients with MDD and 135 HCs were included in neuroimaging methylation analysis. Pearson's partial correlation analysis was used to estimate the correlation between cortical thickness of brain regions and DNA methylation levels of the loci.

Results. In total, 2018 differentially methylated probes (DMPs) and 351 differentially methylated regions (DMRs) were identified. DMP-related genes were enriched in two networks involved in the central nervous system. In neuroimaging analysis, patients with MDD showed cortical thinning in the prefrontal regions and cortical thickening in several occipital regions. Cortical thickness of the left ventrolateral prefrontal cortex (VLPFC, i.e. pars triangularis) was negatively correlated with eight DMPs associated with six genes (*EML6*, *ZFP64*, *CLSTN3*, *KCNMA1*, *TAOK2*, and *NT5E*).

Conclusion. Through combining DNA methylation and neuroimaging analyses, negative correlations were identified between the cortical thickness of the left VLPFC and DNA methylation levels of eight DMPs. Our findings could improve our understanding of the pathophysiology of MDD.

Introduction

Major depressive disorder (MDD), a common psychiatric disorder with a lifetime prevalence of approximately 16%, severely diminishes individuals' quality of life and limits their functioning in family, work, and social lives (Kessler et al., 2007; Kupfer, Frank, & Phillips, 2012). As the neurobiological etiology of MDD, alterations in monoaminergic neurotransmission, dysfunction of neural circuits involved in emotion and reward processing, disturbances in the hypothalamic–pituitary–adrenal (HPA) axis, and changes in neural–immune interactions have also been suggested (Han & Ham, 2021; Kupfer et al., 2012; Malhi & Mann, 2018). The genetic heritability of MDD is estimated to be approximately 37% (Flint & Kendler, 2014), and genetic makeup can determine the risk of MDD through its genetic influences on the aforementioned neurobiological mechanisms in an interactive manner with psychosocial environmental factors such as childhood maltreatment or stressful life events (Klengel & Binder, 2013).

Regarding the etiology of MDD, gene-environmental interactions suggest that the impacts of psychosocial environmental exposure may be highly dependent on one's genetic vulnerability, which, in turn, can regulate the neurobiological mechanisms of response or coping with stressful stimuli such as early life adversities (Klengel & Binder, 2013). Epigenetic mechanisms such as DNA methylation are deeply involved in the fine modulation of the complex interplay between genes and environments through their pivotal role as mediators of the effects of adverse environmental factors on the genome in MDD (Lopizzo et al., 2015). DNA methylation, particularly methylation changes within promoter and enhancer regions of the gene, has been reported to have long-term effects on the transcription of genes involved in the HPA axis (e.g. *FKBP5*, *NR3C1*) (Efstathopoulos et al., 2018; Humphreys et al., 2019; Klinger-König et al., 2019), neuroplasticity (e.g. *BDNF*) (Ferrer et al., 2019; Januar, Ancelin, Ritchie, Saffery, &

© The Author(s), 2024. Published by Cambridge University Press

Ryan, 2015), and monoaminergic neurotransmission (e.g. *SLC6A4*) (Kang et al., 2013; Schneider et al., 2018) in an interactive manner with exposure to stressful life events in depression. More recently, alterations in DNA methylation profiles in response to psychosocial environmental factors have been found in patients with MDD not only at the specific candidate gene level, but also at an epigenome-wide level (Li, Morrison, Turecki, and Drevets, 2022). A recent epigenome-wide association studies (EWAS) by Aberg et al. (2020) found that DNA methylation loci within the serotonin receptor ionotropic 3, subunit c (*HTR3C*) gene were associated with the diagnosis of MDD and a significant overlap of EWAS findings between blood and postmortem brain tissue.

Structural and functional alterations in neural circuits influenced by genetic predispositions may mediate the association between genetic variations and development of MDD (Cattarinussi, Delvecchio, Sambataro, & Brambilla, 2022; Kim, Ham, & Han, 2019; Zhang, Mellor, & Peng, 2018). For epigenetic markers, a growing body of evidence has shown that variations in DNA methylation are associated with structural changes in the brains of patients with MDD (Wheater et al., 2020). For example, Tozzi et al., reported that DNA methylation of the *FKBP5* gene intron, its genetic variation plays a pivotal role in HPA axis regulation through modulation of glucocorticoid receptor sensitivity, is associated with gray-matter concentration in the inferior frontal gyrus, which corresponds to the ventrolateral prefrontal cortex, in patients with MDD (Tozzi et al., 2018). Our previous study also reported that DNA methylation of the serotonin transporter gene (i.e. *SLC6A4*) was inversely correlated with the structural connectivity of the body of the corpus callosum in patients with MDD (Won et al., 2016). However, most previous epigenetic neuroimaging studies on MDD have explored the potential relationship between neuroimaging markers and DNA methylation of specific candidate genes based on *a priori* hypothesis regarding the pathophysiology of MDD, rather than on EWAS-based systematic selection of candidate genes (Chiarella et al., 2020; Kaufman et al., 2018; Yrondi et al., 2021).

Therefore, in this study, we aimed to perform comprehensive epigenetic profiling using EWAS to identify novel epigenetic loci associated with the pathophysiology of MDD using a sample of patients with MDD and healthy controls (HCs). We also explored the differences in profiles regarding copy number alterations (CNAs) and gene networks between the two groups. After exploring significant epigenetic loci at the EWAS level as a neuroimaging-epigenetic study, we also investigated the potential correlation between epigenetic loci and cortical gray matter thickness to examine the potential contribution of epigenetic modifications to brain structural changes in MDD.

To delineate the brain structural signatures influenced by individual epigenomic profiles, we chose the atlas-based cortical thickness of the whole brain as the neuroimaging parameter in the present study. Among the widely studied cortical endophenotypes (i.e. cortical thickness, surface area, and local gyrification index), cortical thickness has a unique genetic origin (Panizzon et al., 2009) and is strongly correlated with age-related trajectories (Hogstrom, Westlye, Walhovd, & Fjell, 2013), which are associated with the pathophysiology of MDD (Miles et al., 2021). Furthermore, cortical thickness is one of the most intensively studied neuroimaging parameters in relation to genetic factors, such as polygenic risk score (Cattarinussi et al., 2022; Miles et al., 2021) and DNA methylation (Freytag et al., 2017; Gonzales et al., 2023) in MDD.

Materials and methods

Study participants

In this study, 350 patients with MDD (118 males and 232 females; 41.48 ± 14.80 years) and 161 HCs (58 males and 103 females; 39.08 ± 13.87 years) were included. Patients with MDD were recruited between July 2015 and August 2021 from the outpatient psychiatric clinic of the Korea University Anam Hospital in Seoul, Republic of Korea. The present study used a combination of two study samples: one study collected clinical and genomic data to identify antidepressant treatment response-related biomarkers, and the second study collected brain MRI data in addition to the aforementioned data (Han et al., 2020a). Thus, among the total of 350 patients with MDD and 161 HCs, 234 patients with MDD and 135 HC underwent additional brain MRI scans. A standardized clinical interview using a Structured Clinical Interview for the fifth edition of the Diagnostic and Statistical Manual of Mental Disorders was conducted to diagnose MDD (First, Williams, Karg, & Spitzer, 2016). Two board-certified Korean psychiatrists conducted the interviews (K.M. Han & B.J. Ham). This study included patients whose diagnoses were confirmed by both psychiatrists. The HCs were recruited via advertisements from the community. A total of 161 HCs were assessed by two board-certified psychiatrists who found no evidence of current or previous psychiatric illness. The following criteria, described in a previous paper, were applied to both groups for sample exclusion (Han et al., 2020b): (i) comorbidity of any other major psychiatric disorders (including personality and substance use disorders), (ii) MDD with psychotic features, (iii) acute patients with homicidal or suicidal thoughts who needed inpatient care, (iv) current or previous major medical illness, (v) current or previous neurological disease, and (vi) any contraindication for MRI. Depressive symptom severity was evaluated using the 17-item Hamilton Depression Rating Scale (HDRS) (Hamilton, 1960). The duration of illness was assessed using a life chart methodology. The Edinburgh handedness test was used to determine whether each participant was right-handed (Oldfield, 1971). All participants were confirmed to have Korean ancestry within the past three generations via self-report. The study protocol was approved by the Institutional Review Board (IRB) of the Korea University Anam Hospital (2017AN0185). All the participants provided written informed consent to participate in the study. For a given sample size (n = 511; 2:1 case:control ratio), DNA methylation differences of 2% and 5% reached statistical power of 42% and 72%, respectively. Statistical power was calculated using the pwrEWAS R package (online Supplementary Fig. S1) (Graw, Henn, Thompson, & Koestler, 2019)

Quality control and pre-processing of DNA Methylation data

The Infinium HumanMethylationEPIC BeadChip (Illumina Inc., San Diego, CA, USA) was used to estimate DNA methylation levels (online Supplementary Materials). For signal intensity values and pre-processing, the ChAMP R package was applied to the Illumina Intensity Data files (Tian et al., 2017). A β-value was used, which coded unmethylated as 0 and fully methylated as 1, to express the methylation level of each probe. Samples with a high proportion of poor-quality probes (>0.1) were excluded. We performed principal component analysis (PCA) to check for outliers that could confound the results among the samples. Probes were eliminated using the following

https://doi.org/10.1017/S0033291724000709 Published online by Cambridge University Press

criteria: (i) detection p-value >0.01 probes, (ii) bead count <3 in at least 5% of the samples, (iii) annotated as SNP-associated probes (Zhou, Laird, & Shen, 2017), (iv) located on the sex chromosome, (v) multi-hit CpG sites (Nordlund et al., 2013), and (vi) non-CG probes. β-mixture quantile normalization (BMIQ) was used to correct the technical batch resulting from differences in the Infinium probe type (Teschendorff et al., 2013). Singular value decomposition (SVD) was used to identify technical batches and covariates. The batch effect correction was conducted using the ComBat algorithm (Johnson, Li, & Rabinovic, 2007). We estimated the white blood cell type composition using the FlowSorted.Blood.EPIC R package (online Supplementary Materials) as differences in white blood cell type composition between samples may act as confounding factors.

MRI data acquisition and neuroimaging processing

T1-weighted images of the participants were obtained using a 3.0-Tesla TrioTM whole-body imaging system (Siemens Healthcare GmbH, Erlangen, Germany) at the Korea University MRI Center. The T1-weighted images were acquired parallel to the anterior-commissure–posterior-commissure line using the 3D T1-weighted magnetization-prepared rapid gradient-echo (MP-RAGE) sequence with the following parameters: repetition time (TR), 1900 ms; echo time (TE), 2.6 ms; field of view, 220 mm; matrix size, 256 × 256; slice thickness, 1 mm; number of coronal slices, 176 (without gap); voxel size, $0.86 \times 0.86 \times 1\ mm^3$; flip angle, 16°; and number of excitations, 1. The T1-weighted MRI neuroimaging analysis included 234 of 350 patients with MDD and 135 of 161 HCs. The gray matter thickness of each cortical region was obtained from the participants' T1 images using the FreeSurfer 6.0 version (Laboratory for Computational Neuroimaging, Athinoula A. Martinos Center for Biomedical Imaging, Charlestown, MA, USA; http://surfer.nmr.mgh.harvard.edu). The FreeSurfer provides a 3D-cortical surface reconstruction model and entails automated procedures for the calculation of cortical thickness, including automatic segmentation of gray/white-matter boundaries, smoothing of the cortical map, and parcellation of cortical regions based on the atlas, as described previous literatures (Dale, Fischl, & Sereno, 1999; Fischl, Liu, & Dale, 2001; Fischl et al., 2002; Fischl, Sereno, & Dale, 1999; Fischl et al., 2004; Ségonne, Pacheco, & Fischl, 2007). Cortical gray matter thickness was determined as the shortest distance between the gray/white matter and pial surfaces measured in millimeters (mm) (Han et al., 2020b). The cortical map was smoothed using a Gaussian kernel with a full width at half maximum of 20 mm for all cortical analyses (Han et al., 2020b). The thicknesses of the 74 cortical gyri and sulci were calculated, and we then used the gray matter thickness value of the 38 cortical gyri in each hemisphere based on the atlas by Destrieux, Fischl, Dale, and Halgren (2010). The total intracranial cavity volume (TICV) was automatically calculated using the FreeSurfer software.

Differentially methylated positions and regions

Differentially methylated probes (DMPs) and differentially methylated regions (DMRs) were evaluated in patients with MDD and HCs. Treatment was based on covariates consisting of cell type heterogeneity, age, sex, and two principal components (PCs). Two PCs were included to correct for unknown biases. DMPs were identified using the limma R package (Ritchie et al., 2015). Bonferroni corrected p-value was applied to the DMP results (p-value $\leqslant 0.05/(734\,794\ \text{probes}) = 6.80 \times 10^{-8}$). We used the dmrff R package, which is based on inverse variance-weighted statistics (Suderman et al., 2018), to identify DMR. Significant DMR was considered based on the following criteria: (i) distance between probes in a region $\leqslant$300 bp, (ii) number of probes in a region $\geqslant$2, (iii) each region should be related with at least one gene, and (iv) false discovery rate (FDR) $\leqslant$0.05. The genomic coordinates of DMPs and DMRs were represented based on the GRCh38/hg38 reference genome.

Copy number alteration

CNA was performed using the ChAMP R package, which is based on the circular binary segmentation (CBS) method using HCs as a reference (Olshen, Venkatraman, Lucito, & Wigler, 2004; Tian et al., 2017). Focal- and arm-level events that contained frequent gains or losses in the MDD group were determined using the Genomic Identification of Important Targets in Cancer 2.0 (GISTIC) algorithm. The genomic coordinates of the CNAs are represented based on the GRCh38/hg38 reference genome. Copy numbers >0.5 or < −0.5 were defined as copy number gains or losses, respectively.

Network analysis

Network analysis was performed using the Ingenuity Pathway Analysis (IPA) software (Ingenuity Systems, Redwood City, CA, USA) with genes that corresponded to significant DMPs. The $\Delta\beta$ values of DMPs were used to determine how each gene affects the integrated network, containing estimations of direct and indirect connections as well as experimentally observed relationships. The score for each network was calculated based on the set of focused genes in the network.

Neuroimaging analysis

Neuroimaging analyses were performed in two steps: First, one-way analysis of covariance (ANCOVA) was conducted adjusting for sex, age, TICV, and years of education to identify the difference in cortical thickness between the MDD and HC groups. The Benjamini–Hochberg (BH) approach was used to correct multiple testing error (the false discovery rate [FDR] $\leqslant$0.05) for the comparison of the cortical thickness between the two groups. Second, Pearson's partial correlation analysis was used to determine whether a relationship exists between the significant CpG sites and the thickness of the cortical regions, which showed significant differences between the two groups, for the neuroimaging-epigenetic correlation analysis. The only significant DMPs were included in the correlation analysis (i.e. p-value $\leqslant 6.80 \times 10^{-8}$). Correlation analyses were performed for the MDD and HC groups using the following covariates: Sex, age, TICV, years of education, HDRS score, medication status (coded drug-naïve patients as 0 and medicated patients as 1), and illness duration were used as covariates for the MDD group. Illness duration, HDRS score, and medication status were excluded from the covariates in the HC group, as described in our previous study (Han et al., 2022). The BH approach was also applied in the neuroimaging-epigenetic correlation analyses (FDR $\leqslant$ 0.05). CpG sites derived from the neuroimaging-epigenetic analysis were used to confirm potential co-methylation effects using coMET R package (Martin, Yet, Tsai, & Bell, 2015) (see online Supplementary Materials for detail).

https://doi.org/10.1017/S0033291724000709 Published online by Cambridge University Press

The correlations between the DNA methylation level of the CpG sites and HDRS scores were analyzed to further investigate the relationship between DNA methylation level and MDD severity using the Spearman rank correlation coefficient. Considering the patients in remission, a linear regression method was applied to adjust for the remission status on DNA methylation level before conducting the correlation analysis. R 4.0.3 environment was applied for all statistical analyses.

Results

Differentially methylated positions and regions

We performed a differential methylation analysis in 350 patients with MDD and 161 HCs. Age, years of education, and HDRS scores were significantly different between the MDD and HC groups (p-value ⩽0.05; Table 1). After quality control, 734 794 CpG sites remained and were used for differential methylation analysis.

A total of 2018 CpG sites were identified as significant DMPs with Bonferroni-corrected p-value (p-value $\leqslant 6.80 \times 10^{-8}$) (online Supplementary Table S1). These DMPs (1128 hypermethylated and 890 hypomethylated sites) were associated with 1474 unique genes, including 333 MDD-related genes (Fig. 1*a*, *b*). The top 20 DMPs are presented in Table 2 and highlighted in Fig. 1*b*. Among them, cg03009437 (chr22:31276850; *LIMK2*), cg07670259 (chr17:2613677; *PAFAH1B1*), and cg13128596 (chr11:104969131; *CASP4*) were associated with MDD-related genes with p-values of 2.84×10^{-15}, 3.96×10^{-15}, and 4.30×10^{-15}, respectively (Gao et al., 2020; Hall et al., 2018; Nagel et al., 2018).

The functional genomic and CpG island regions of 2018 significant DMPs were separated into hypermethylated and hypomethylated DMPs. Among the 2018 DMPs, 560 of the 1128 (49.65%) hypermethylated DMPs were aligned to the body region of the gene (Fig. 1*c*). The second highest number of hypermethylated DMPs (340 of 1128 DMPs, 30.14%) were aligned within the intergenic region (IGR) (Fig. 1*c*). Conversely, 27.4% of the hypomethylated DMPs were located at 200 bp upstream of the transcript start site (TSS200), 17.64% at 1500 bp upstream of the transcript start site (TSS1500), 15.05% in the gene body, 14.27% in the 5′ untranslated region (5′ UTR), 13.82% in the first exons, 11.12% in the IGR, 0.67% in the 3′ untranslated region (3′ UTR), and no DMPs in exon boundaries (Fig. 1*c*). Interestingly, we found that 64.1% of the hypermethylated DMPs were located in the open-sea region, whereas 73.6% of the hypomethylated DMPs were located in the CpG island region, which is highly distributed in mammalian gene promoters (Fig. 1*d*) (Saxonov, Berg, & Brutlag, 2006). In summary, hypermethylated DMPs were found more frequently in the gene body region and IGR, whereas hypomethylated DMPs were found more frequently in promoter-associated regions. A previous study revealed that increased DNA methylation levels in the gene body regions may increase gene expression (Laurent et al., 2010). Thus, our findings suggest that MDD-related genes are upregulated through epigenetic modifications in patients with MDD.

Table 1. Demographic and clinical characteristics of patients with MDD and HCs

Characteristics	MDD (n = 350)	HC (n = 161)	P-value (t, χ^2)
Age (mean ± S.D.)	41.76 ± 14.77	38.41 ± 13.94	0.016[a] (t = 2.426)
Sex (female/male)	232/118	104/57	0.763[b] (χ^2 = 0.140)
Education years (mean ± S.D.)	13.11 ± 3.21	15.04 ± 2.26	<0.001[a] (t = − 7.802)
HDRS-17 score (mean ± S.D.)	16.41 ± 6.64	0.93 ± 1.69	<0.001[a] (t = 19.155)
Remission state/depressive state	38/312	NA	NA
Illness duration (mean ± S.D.) (months)	28.64 ± 28.82	NA	NA
Drug-naive/drug-treated patients (n)	106/244	NA	NA
Medication (*n*)			
Antidepressants			
SSRI	97	NA	NA
SNRI	55		
NDRI	5		
NaSSA	22		
Etc	10		
Combination of AD	55		
Antipsychotics			
None	166		
AP	58		
Combination of AP	20		

[a]p values for comparisons of age, years of education, HDRS scores, and TICV were obtained using independent t tests.
[b]p-values for sex distribution were obtained using the chi-square test.
HCs, healthy controls; MDD, major depressive disorder; SD, standard deviation; HDRS-17, 17-item Hamilton Depression Rating Scale; TICV, total intracranial cavity volume; SSRI, selective serotonin reuptake inhibitor; SNRI, serotonin and norepinephrine reuptake inhibitor; NDRI, norepinephrine-dopamine reuptake inhibitor; NaSSA, noradrenergic and specific serotonergic antidepressant; APs, antipsychotics; ADs, antidepressants.

https://doi.org/10.1017/S0033291724000709 Published online by Cambridge University Press

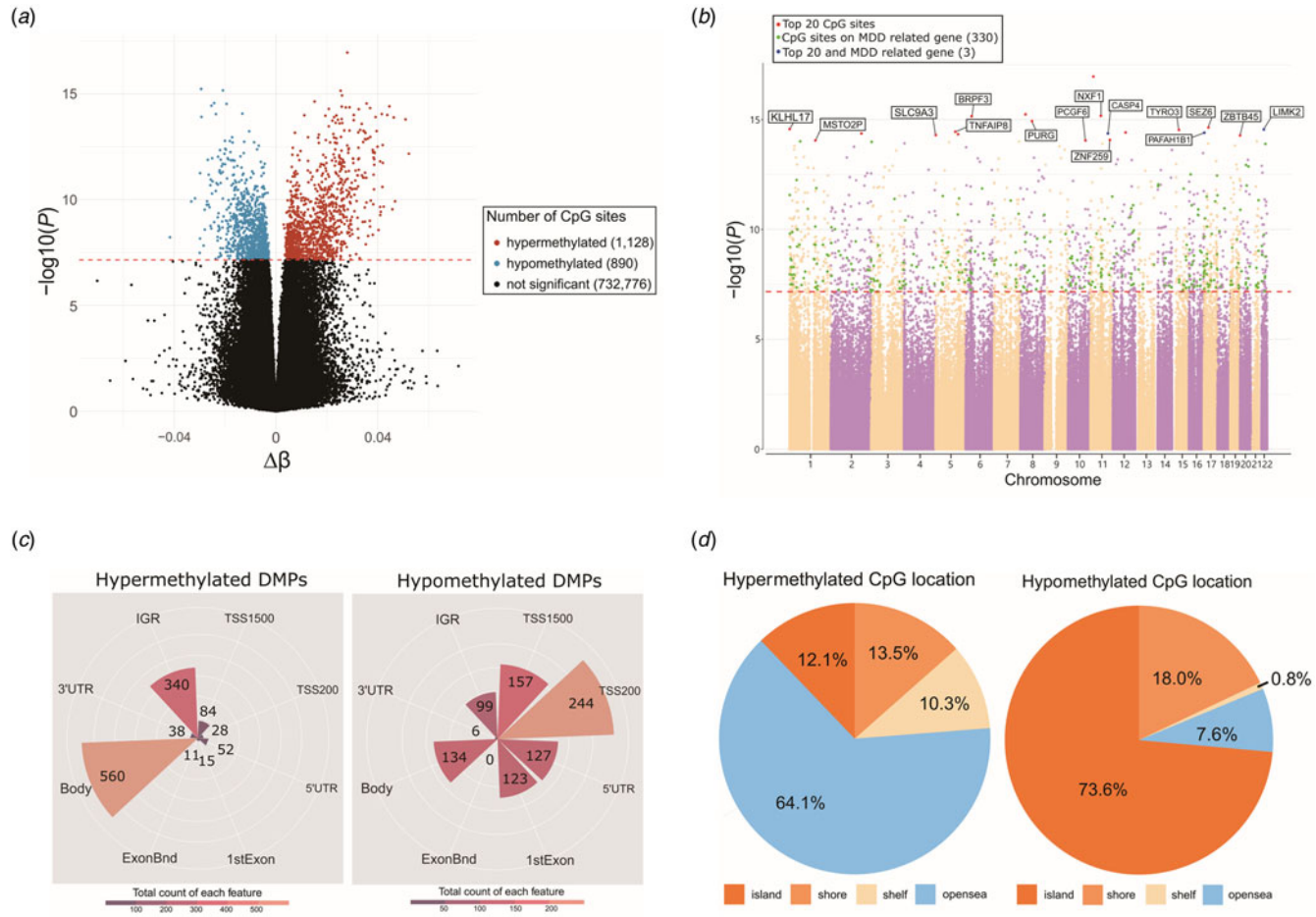

Figure 1. Differentially methylated probes (DMPs) between major depressive disorder (MDD) and healthy control (HC) groups. (a) Volcano plot of all CpG sites. X-axis represents $\Delta\beta$, and y-axis represents −log10(*p*-value). Hypomethylated probes in MDD group are highlighted in blue, whereas hypermethylated probes are highlighted in red. Black dot represents probes that are not significant. The horizontal dashed line at −log10(6.80E − 08) indicates the Bonferroni corrected *p*-value of 0.05. $\Delta\beta$ (delta-beta), the average beta value of MDD patients minus the average beta value of HCs. (b) Manhattan plot of all CpG sites. Y-axis represents −log10(*p*-value), whereas x-axis represents chromosomes. Different colors are used to identify different chromosomes. DMP results were adjusted for sex, age, white blood cell composition and two principal components. The horizontal red dashed line at −log10(6.80E − 08) indicates the Bonferroni corrected *p*-value of 0.05. For the top 20 significant DMPs, 17 CpG sites are labeled with red dots and three CpG sites are labeled with blue dots since they are found in MDD related genes. Among the remaining, a total of 330 green labeled CpG sites are found in MDD related genes. (c) Polar bar plot indicating distributions of functional genomic regions of hypermethylated (left) and hypomethylated (right) DMPs. Colors are illustrated according to the number of probes for each functional genomic region. TSS1500, 200–1500 bp upstream of the transcriptional start site; TSS200, 0–200 bp upstream of the transcriptional start site; 5′UTR, between the transcriptional start site and the ATG start site; 1stExon, first exon; Body, between the ATG and stop codon; 3′UTR, between the stop codon and poly A signal; IGR, intergenic region; ExonBnd, Exon-boundary. (d) Pie chart illustrating distributions of hypermethylated (left) and hypomethylated (right) DMPs according to the CpG island regions. Different color labels are used to distinguish different regions. shelf, 2–4 kb from a CpG island; shore, 0–2 kb from a CpG island; openSea, >4 kb from a CpG island; island, CpG island.

DMRs can capture additional signals from multiple single sites because they collect methylation variations between subsequent probes in an area. A total of 351 DMRs were identified using the criteria described in the Materials and Methods section, after adjusting for sex, age, and two principal components (online Supplementary Table S2). The most significant DMR was located on chromosome 6, which included two CpG sites associated with the gene body region of the *BRPF3* gene (online Supplementary Table S2).

Copy number alteration

To detect CNAs, 350 patients with MDD were analyzed using GISTIC algorithm. A total of 37 gains and 23 losses were identified at FDR $\leqslant 1.0 \times 10^{-4}$ (online Supplementary Fig. S2). Recurring focal CNAs in patients included gains in *HLA-DRB5* on 6p21.32, *HLA-A* and *RNF39* on 6p22.1, olfactory receptor gene family (*OR4K5*, *OR11H2*, *OR4K1*, *OR4K2*, *OR4N2*, *OR11H12*, *OR4Q3*, and *OR4M1*) on 14q11.2, and *HLA-B* on 6p22.33, and losses in *HCG4B* on 6p22.1, *HLA-B* on 6p21.33, *DUSP22* on 6p25.3, *LOC645166* on 1q21.2, and *LOC641298* on 16p12.2 (online Supplementary Table S3).

Gene network analysis

IPA was performed to identify the interactions and networks between the 1474 DMP-related genes. The IPA identified the enrichment of 25 networks involved in multiple diseases and disorders. We found two networks associated with the central nervous system (CNS): A network with a score of 29 was associated with nervous system development and function, organ morphology,

https://doi.org/10.1017/S0033291724000709 Published online by Cambridge University Press

Table 2. Top 20 DMPs obtained from methylation analysis of patients with MDD

CpG site	*p*-Value[a]	Δβ	CHR	Position[b]	Gene	Functional region[c]	CGI region[d]	MDD related gene[e]
cg20996545	1.11×10^{-17}	0.028	11	17 226 920		IGR	Shore	
cg21604516	5.80×10^{-16}	−0.029	8	31 032 953	*PURG*	TSS200	Opensea	
cg03901462	6.79×10^{-16}	−0.021	11	62 805 402	*NXF1*	1stExon	Island	
cg16525439	7.09×10^{-16}	0.025	6	36 211 131	*BRPF3*	Body	Opensea	
cg22549556	1.18×10^{-15}	0.026	8	69 130 039		IGR	Opensea	
cg19527233	2.29×10^{-15}	0.015	17	28 960 994	*SEZ6*	Body	Opensea	
cg09789536	2.71×10^{-15}	−0.024	1	960 846	*KLHL17*	Body	Island	
cg03009437	2.84×10^{-15}	0.036	22	31 276 850	*LIMK2*	Body	Shore	*LIMK2*
cg24491553	2.96×10^{-15}	−0.019	15	41 559 012	*TYRO3*	TSS200	Shore	
cg17432189	3.58×10^{-15}	−0.025	5	119 268 565	*TNFAIP8*	TSS200	Shore	
cg27272293	3.87×10^{-15}	0.045	12	76 137 227		IGR	Opensea	
cg07670259	3.96×10^{-15}	0.026	17	2 613 677	*PAFAH1B1*	5'UTR	Opensea	*PAFAH1B1*
cg13128596	4.30×10^{-15}	0.029	11	104 969 131	*CASP4*	TSS1500	Opensea	*CASP4*
cg15779295	4.34×10^{-15}	0.027	2	183 260 624		IGR	Island	
cg05521474	4.65×10^{-15}	0.037	5	135 746 507		IGR	Opensea	
cg17836790	5.10×10^{-15}	0.021	5	500 450	*SLC9A3*	Body	Island	
cg12271800	5.27×10^{-15}	0.033	19	58 517 397	*ZBTB45*	Body	Island	
cg19345149	8.55×10^{-15}	−0.013	11	116 788 159	*ZNF259*	TSS200	Island	
cg07222421	8.92×10^{-15}	0.042	1	155 748 857	*MSTO2P*	Body	Shelf	
cg25481680	8.95×10^{-15}	−0.024	10	103 351 121	*PCGF6*	5'UTR	Island	

[a]Bonferroni corrected *p*-value (⩽0.05/(734 794 probes) = 6.80E − 08).
[b]UCSC GRCh38/hg38.
[c]CpG sites located in functional genomic regions, TSS1500, 200–1500 bases upstream of the transcriptional start site; TSS200, 0–200 bases upstream of the transcriptional start site; 5′UTR, between the transcriptional start site and ATG start site; 1stExon, first exon; Body, between ATG and stop codon; IGR, intergenic region.
[d]CpG sites located on CpG islands, Shelf, 2–4 kb from a CpG island; Shore, 0–2 kb from a CpG island; OpenSea, >4 kb from a CpG island; Island, CpG island.
[e]MDD-related genes were extracted from the GWAS catalog (https://www.ebi.ac.uk/gwas/) and PubMed (https://pubmed.ncbi.nlm.nih.gov/).
DMP, differentially methylated probe; MDD, major depressive disorder; Δβ (delta-beta), the average beta value of MDD patients minus the average beta value of HCs; CGI, CpG island.

and tissue morphology (online Supplementary Fig. S3a). Another network, with a score of 29, was associated with developmental disorders, hereditary disorders, and neurological diseases (online Supplementary Fig. S3b).

Cortical thickness alterations

In the neuroimaging analysis, 234 of 350 patients with MDD and 135 of 161 HCs were included (online Supplementary Table S4). Comparisons of 76 cortical thickness of the bilateral hemispheres between the MDD and HC groups showed that four significantly increased cortical regions and three significantly decreased cortical regions with FDR ⩽ 0.05 (online Supplementary Table S5). Patients with MDD showed significantly decreased cortical thicknesses in the left pars triangularis (FDR = 0.046), right transverse frontopolar gyrus (FDR = 0.018), and middle frontal gyrus (FDR = 0.018). The patient group also showed significantly increased cortical thickness in several occipital regions, including the bilateral lingual gyri (right: FDR = 0.020; left: FDR = 0.046), left superior occipital gyrus (FDR = 0.021), and the right cuneus (FDR = 0.023) (online Supplementary Table S6).

We performed an ad hoc analysis to investigate the potential correlation between cortical thickness of the left pars triangularis and illness duration or depression severity. In Pearson's partial correlation analysis, we observed a weak but significant negative correlation between illness duration and the thickness of the left pars triangularis in the MDD group ($r = -0.156$, p-value = 0.019), with age, sex, TICV, years of education, medication, and the HDRS score as covariates. However, we did not find any significant correlation between HDRS score and cortical thickness in the MDD group.

Correlation between DNA methylation and cortical thickness

Correlation analyses were conducted using the β values of 2018 significant DMPs and the thicknesses of 76 cortical regions. Within seven cortical regions that showed different cortical thickness between the MDD and HC groups, eight CpG sites had significant correlations at FDR ⩽ 0.05 (Table 3). For these eight CpG sites, the cortical thickness of the left pars triangularis showed negative correlations with cg09705759 (r = −0.213, FDR = 0.022), cg14706523 (r = −0.213, FDR = 0.031), cg02593636 (r = −0.231, FDR = 0.034), cg26929161 (r = −0.229, FDR = 0.038), cg01490772 (r = −0.217, FDR = 0.039), cg23644045 (r = −0.227, FDR = 0.043), cg24300703 (r = −0.227, FDR = 0.043), and cg04227758 (r = −0.225, FDR = 0.049) (Table 3) in the MDD group. This relationship was absent in the HC group entirely (Fig. 2). Additionally, we analyzed the correlation between the methylation level of eight CpG sites and HDRS scores in the MDD and HC groups, respectively. Among the eight CpG sites,

https://doi.org/10.1017/S0033291724000709 Published online by Cambridge University Press

Table 3. Correlation between cortical thickness of significant brain regions and DNA methylation levels of eight CpG sites in patients with MDD

Cortical regions	CpG site (functional region[a]; $\Delta\beta$)	CHR	Position[b]	Gene	*r*	*P*-value	FDR[c]
L Pars triangularis	cg09705759 (IGR; 0.008)	4	139 634 378		−0.213	1.22×10^{-3}	0.022
	cg14706523 (Body; 0.008)	2	54 740 436	*EML6*	−0.213	1.23×10^{-3}	0.031
	cg02593636 (IGR; 0.029)	12	10 505 730		−0.231	4.45×10^{-4}	0.034
	cg26929161 (Body; 0.035)	20	52 084 727	*ZFP64*	−0.229	5.04×10^{-4}	0.038
	cg01490772 (TSS1500; −0.003)	12	7 129 997	*CLSTN3*	−0.217	1.02×10^{-3}	0.039
	cg23644045 (Body; 0.013)	10	77 527 229	*KCNMA1*	−0.227	5.62×10^{-4}	0.043
	cg24300703 (Body; 0.008)	16	29 979 474	*TAOK2*	−0.227	5.69×10^{-4}	0.043
	cg04227758 (Body; 0.017)	6	85 476 633	*NT5E*	−0.225	6.42×10^{-4}	0.049

[a]CpG sites locate in functional genomic regions, TSS1500, 200–1500 bases upstream of the transcriptional start site; Body, between the ATG and stop codon; IGR, intergenic region.
[b]UCSC GRCh38/hg38.
[c]Benjamini–Hochberg (BH) approach was applied (FDR ⩽ 0.05).
MDD, major depressive disorder; $\Delta\beta$ (delta-beta), the average beta value of MDD patients minus the average beta value of HCs; FDR, false discovery rate; L, left hemisphere.

cg09705759 showed a positive correlation with the HDRS scores (r = 0.120, p-value = 0.025), whereas cg01490772 showed a negative correlation with the HDRS scores (r = −0.237, p-value = 8.03×10^{-6}). Those relationships were not observed in the HC group, indicating that these CpG sites may have potential as epigenetic markers for assessing MDD severity (online Supplementary Fig. S4).

Discussion

In this study, we performed a comprehensive analysis to examine the association between genome-wide DNA methylation and structural changes in the brain of patients with MDD. The main strength of this study was the investigation of novel epigenetic loci and their relationship with cortical thickness in patients with MDD. We found 2018 candidate CpG sites and 351 regions. Interestingly, 8 of the 2018 CpG sites from the EWAS results showed significant negative correlations with the cortical thickness of the left pars triangularis, which corresponds to the ventrolateral prefrontal cortex (VLPFC) in patients with MDD. The present study makes an important contribution to the understanding of the pathophysiology of MDD regarding the interactions between epigenetic makeup, structural brain changes, and the disease.

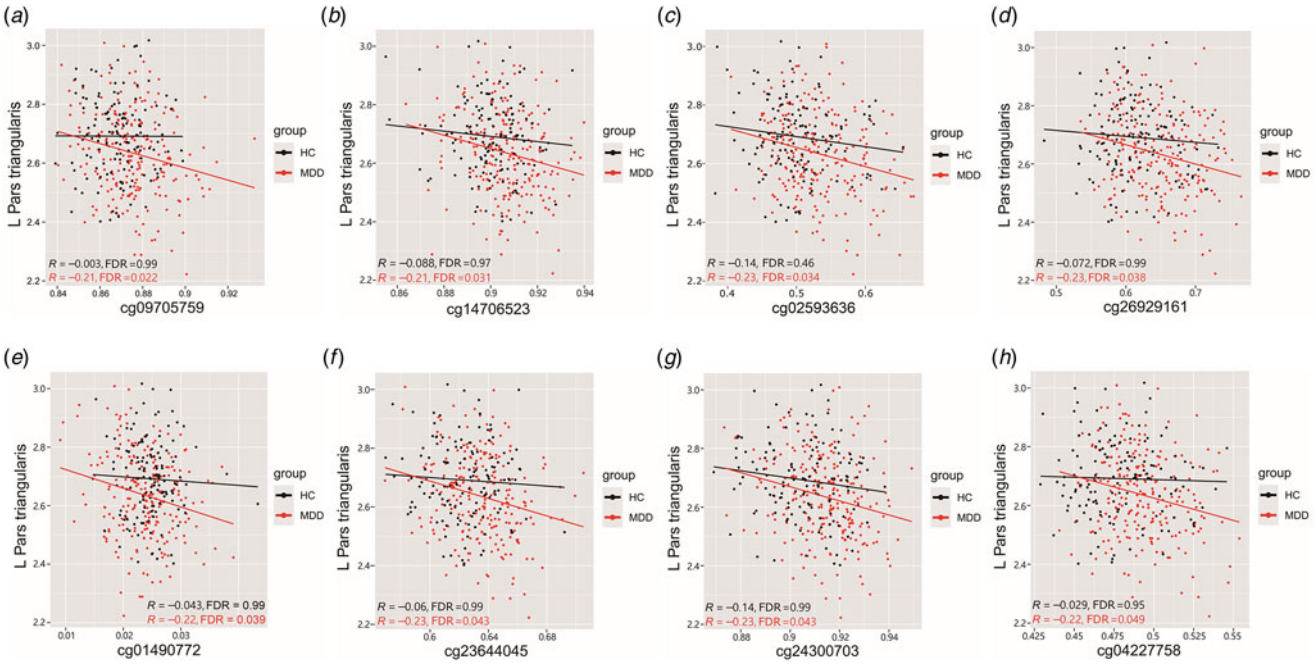

Figure 2. Scatter plots of Pearson's partial correlation analysis between brain cortical thickness and differentially methylated probes (DMPs). Red dots/lines indicate MDD group and black dots/lines indicate HC group. Colored line represents the correlation between cortical thickness of brain region and methylation level of CpG sites. Each plot showed significant negative correlations between the left pars triangularis and (a) cg09705759, (b) cg14706523, (c) cg02593636, (d) cg26929161, (e) cg01490772, (f) cg23644045, (g) cg24300703, and (h) cg04227758. Cortical thickness was adjusted for age, sex, education year, total intracranial cavity volume, illness duration, HDRS score, and medication status. Methylation level was adjusted for age, sex, PC1, and PC2. Pearson correlation coefficients and *p*-values are indicated for both groups. MDD, major depressive disorder; HC, healthy control; L, left hemisphere; R, Pearson's partial correlation coefficient; HDRS, 17-item Hamilton Depression Rating Scale; PC, principal component.

https://doi.org/10.1017/S0033291724000709 Published online by Cambridge University Press

Of the top 20 DMP-related genes, the nuclear RNA export factor 1 (*NXF1*) gene has been identified as a positive regulator of the IRF5 signaling pathway that was involved in various autoimmune diseases, such as inflammatory bowel disease and multiple sclerosis (Kaur, Lee, Chow, & Fang, 2018). Seizure-related gene 6 (*Sez6*), another top DMP-related gene, encodes a transmembrane protein that modulates synaptic plasticity in the cortex and hippocampus (Gunnersen et al., 2007). *Sez6* is involved in psychiatric disorders, including autism spectrum disorder (ASD), childhood-onset schizophrenia, and bipolar disorder (BD) (Ambalavanan et al., 2016; Chapman et al., 2015; Xu et al., 2013). Given the neural–immune interactions and synaptic plasticity are deeply involved in the etiology of MDD (Barnes, Mondelli, & Pariante, 2017; Duman, Aghajanian, Sanacora, & Krystal, 2016; Han & Ham, 2021; Troubat et al., 2021), our results suggest that *NXF1* and *Sez6* methylation may play an important role in the pathophysiology of MDD. Among the other top DMP-related genes, LIM kinase 2 (*LIMK2*), a gene that regulates cortical development and was reported to be associated with schizophrenia by a recent EWAS in the Han Chinese population (Li et al., 2021). A previous study also reported its up-regulation in deep layer three pyramidal cells in the dorsolateral prefrontal cortex in patients with schizophrenia (Datta, Arion, Corradi, & Lewis, 2015). Bromodomain and PHD finger containing protein 3 (*BRPF3*), which is involved in the regulation of the histone acetyltransferase activity and substrate specificity, was reported to be associated with both, MDD in a recent large-scale whole-exome sequencing study (Zhou et al., 2021) and antidepressant response in patients with MDD (Kang et al., 2020). *PAFAH1B1*, also known as *LIS1*, encodes a critical mediator of neuronal migration in brain development (Sudarov et al., 2018) and is suggested to be related with chronic mental illness such as schizophrenia and BD (Cukkemane et al., 2021; Tabarés-Seisdedos et al., 2006). This gene is also deeply involved in synaptic function and plasticity of mature CA1 neurons in the hippocampus (Sudarov et al., 2018). A Kelch-like 17 (*KLHL17*) gene, which encodes a neuron-specific F-actin binding protein, is known to regulate dendritic spine morphology or plasticity and be associated with neurodevelopment disorders such as intellectual disability and ASD (Hu, Huang, & Hsueh, 2020; Huang, Fang, Kung, & Chen, 2022). *CASP4* gene encodes a caspase-4, which plays a critical role in inflammatory responses, secretion of interleukin (IL)-1b and IL-18 (Kajiwara et al., 2014) and is reported to be associated with schizophrenia and BD in a human study (de Baumont et al., 2015). A previous mouse study also suggested that this gene contributes to the pathogenesis and cognitive impairment in Alzheimer's disease (Kajiwara et al., 2016). The exact function of *PURG*, which encodes a kind of purine-rich element-binding protein, is not well understood, several genome-wide association studies have reported that *PURG* is associated with cognitive performance and intelligence (Hill et al., 2019; Kang et al., 2023; Lee et al., 2018).

A significantly hypermethylated region was identified in the gene body region of the histone deacetylase 3 (*HDAC3*) gene, which is a member of the class I HDACs (Park & Kim, 2020). Overexpression of *HDAC3* has been reported to accelerate oxidative stress-induced neurodegenerative processes (Bardai & D'Mello, 2011). Furthermore, previous studies have reported that *HDAC3* is associated with the pathophysiology of Parkinson's and Alzheimer's disease (Choi et al., 2015; Mahady et al., 2018). Another significant DMR was found in the promoter hypomethylation of the orphan G protein-coupled receptor 12 (*GPR12*) gene, which plays a critical role in cortical development (Ignatov et al., 2003). A previous study has reported that *GPR12* is upregulated in the microglia through a neuroinflammation process (Bédard, Tremblay, Chernomoretz, & Vallières, 2007). Given the suggested roles of these genes, epigenetic modifications may be associated with the pathophysiology of MDD.

We found significant CNAs within several genes, including the ring finger protein 39 (*RNF39*) and olfactory receptor gene families. According to a previous study, the hypomethylation of *RNF39*-containing DMR is associated with the development of PTSD after traumatic stress exposure (Rutten et al., 2018). The olfactory receptor gene family, located at 14q11.2, is strongly associated with ASDs and an earlier age of Alzheimer's disease (Gibitova et al., 2022; Shaw et al., 2011). Interestingly, the human leukocyte antigen (HLA) regions contain the most abundant focal gain and loss regions in the present study. Recently, there has been growing evidence that inflammatory markers or autoimmune diseases that play a role in the etiology of MDD are correlated with highly polymorphic HLA regions (Gough & Simmonds, 2007; Osimo et al., 2020). Although significant alterations were observed in our study, these results warrant further investigation.

Given the epigenetic variations, we identified two gene networks associated with the CNS. The first gene network included the NF-κB complex with multiple indirect interactions. NF-κB plays a crucial role in inflammatory and structural plasticity in the mature brain (Dresselhaus & Meffert, 2019). The second gene network included Tumor necrosis factor-a-induced protein 8 (*TNFAIP8*) and TYRO3 protein tyrosine kinase (*TYRO3*), the top-ranked DMP-related genes. *TNFAIP8* is essential for maintaining immune homeostasis via regulating IκBα/NF-κB and PI3K/Akt signaling pathways (Xue et al., 2020). Downregulation of *TYRO3* has been implicated in loss of stress resistance (e.g. hypoxia and neurotransmitter overstimulation) and neurodevelopmental diseases (Pierce & Keating, 2014; Zhang et al., 2023). Therefore, the complex interactions of these genes may be associated with the pathophysiology of MDD through their involvement in structural alterations and neuroinflammatory processes in the brain.

In this study, we observed significant cortical thinning of the prefrontal cortex (PFC), including the left pars triangularis, right transverse frontopolar, and middle frontal gyri, and cortical thickening in several occipital regions in the MDD group. A reduction in MDD-associated cortical thickness in the PFC has been consistently reported in numerous MRI studies (Schmaal et al., 2017; Suh et al., 2019). For example, a previous meta-analysis by Schmaal et al. (2017), using MRI data from 2148 patients with MDD and 7957 HC volunteers from 20 sites worldwide, reported significant MDD-related thinning of the PFC, including the pars triangularis, middle frontal gyrus, and frontal pole, which corresponds to the results of the present study. In particular, the pars triangularis, which corresponds to the VLPFC and its cortical thinning, was significantly correlated with epigenetic loci in the present study and is deeply involved in the cognitive control of negative emotions and reward processing with regard to the neural circuit dysfunction of MDD (Phillips et al., 2015; Rive et al., 2013).

We examined the association between 2018 DMPs and cortical region thickness, which showed significant differences between the MDD and HC groups, to identify novel epigenetic loci associated with cortical thickness changes in patients with MDD. The reduction in the cortical thickness of the left pars triangularis, which corresponds to the VLPFC, was strongly correlated with

https://doi.org/10.1017/S0033291724000709 Published online by Cambridge University Press

DNA methylation changes in eight CpG sites in the MDD group but not in the HC group. We found that six out of eight CpG sites were associated with *EML6*, *ZFP64*, *CLSTN3*, *KCNMA1*, *TAOK2*, and *NT5E* genes. *CLSTN3* encodes calsyntenin-3, a synaptogenic adhesion molecule that plays an important role in GABAergic and glutaminergic synaptic development (Um et al., 2014). This gene has been reported to be associated with ASDs and schizophrenia via its involvement in brain development (Howes & Onwordi, 2023; Woodbury-Smith et al., 2022). Furthermore, a recent study using maternal peripheral blood samples from 92 participants reported that DNA methylation of *CLSTN3* was associated with postpartum depressive symptoms (Lapato et al., 2019). *EML6* encodes microtubule-associated proteins, which are associated with cytoskeletal function (Shinde et al., 2021), and its genetic expression has been reported to be altered in post-mortem PFC tissue from patients with Alzheimer's disease (Sherva et al., 2023) and postmortem midbrain tissue from those with schizophrenia (Puvogel et al., 2022). *TAOK2* is located in the 16p11.2 chromosomal deletion region, which is known to be associated with ASD and schizophrenia (Richter et al., 2019). This gene has a critical role in brain development through involvement in synaptic and dendritic development (Richter et al., 2019), and its genetic variant was associated with psychosis phenotype, including schizophrenia and BD, in the genome-wide association study (Steinberg et al., 2014), and a most recent EWAS reported that DNA methylation of *TAOK2* was associated with the degree of general psychopathology in childhood (Rijlaarsdam et al., 2023). *KCNMA1* encodes the BK channels, which comprise four α-subunits of the calcium ion-activated potassium channel and play an important role in the synaptic regulation of neuronal excitability (Laumonnier et al., 2006). *KCNMA1* has been reported to be associated with ASD and neurodevelopment disorders (Cheng, Qiu, & Du, 2021), and its de novo mutation was reported to be associated with ASD (Wu et al., 2020). *ZFP64* encodes a co-activator of the Notch signaling pathway (Sakamoto, Tamamura, Katsube, & Yamaguchi, 2008), which is involved in the regulation of neuronal cell proliferation, differentiation, and growth (Ables, Breunig, Eisch, & Rakic, 2011). The potential contribution of the Notch signaling pathway to the predisposition to psychiatric disorders has been reported (Hoseth et al., 2018). Previous studies have reported that *ZFP64* is associated with recurrent MDD (Glahn et al., 2012) and binge eating behavior in BD (Winham et al., 2014). Another significant CpG site, cg04227758, was located in the body region of the *NT5E* gene. The *NT5E* gene encodes ecto-5′-nucleotidase (CD73), which plays a role in converting 5′-adenosine monophosphate (AMP) to adenosine (Lennon, Taylor, Stahl, & Colgan, 1998). Dysregulation of the adenosine metabolism pathway can contribute to the etiology of psychiatric disorders, including ASD, Alzheimer's disease, and MDD (Liu et al., 2019), because it may affect neuronal dysfunction and neurodegeneration via glutamatergic neurotransmission (Cunha, 2016). Previous studies have reported that *NT5E* is associated with diagnosis of BD (Bigdeli et al., 2013) and history of childhood trauma in patients with MDD (Van der Auwera et al., 2018).

An epigenetic modification refers to not only a potentially heritable, but also an environmentally modifiable regulation of gene function and expression by psychosocial stresses particularly for childhood maltreatments (Lopizzo et al., 2015). Furthermore, convergence evidence has shown that this environment-induced alteration in DNA methylation contributes to an individual's predisposition to MDD by impairing brain network development (Wheater et al., 2020). For example, a study by Tozzi et al. (2018) found that DNA methylation of *FKBP5* gene intron seven regions was correlated with the degree of childhood adversity among patients with MDD and high-risk allele of rs1360780, and that DNA methylation was also correlated with reduced gray matter concentration in the prefrontal cortex (i.e. inferior frontal orbital gyrus). Another study suggested that childhood maltreatment was associated with higher DNA methylation levels of the oxytocin receptor (*OXTR*) gene, which was negatively correlated with the gray matter volume of the left orbitofrontal cortex among children (Fujisawa et al., 2019). Considering the potential interplay among epigenetic modifications, early life stress, and brain structural changes with regard to the pathophysiology of MDD (Uchida, Yamagata, Seki, & Watanabe, 2018; Wheater et al., 2020), epigenetic loci associated with the diagnosis of MDD or cortical thickness changes in the present study may have underlying potential interactions with psychosocial environmental factors. However, we did not investigate participants' psychosocial environmental factors, such as early life stress, which might limit our ability to unravel the complex interplay among epigenetic mechanisms, structural brain changes, and the development of MDD.

In a combined neuroimaging-epigenetic analysis, only a subset of epigenetic loci was associated with cortical thickness changes in patients with MDD. Several epigenetic loci can increase an individual's susceptibility to the development of MDD by modulating the pathophysiological pathways of MDD (Penner-Goeke & Binder, 2019). Among these epigenetic loci, some may be involved in neurobiological mechanisms that could impact intermediate neuroimaging phenotypes, such as structural brain changes associated with depression, including synaptic and dendritic development, neuronal cell proliferation, differentiation, growth, and glutamatergic neurotransmission (Uchida et al., 2018; Wheater et al., 2020). Recent large-scale collaborative imaging-genetic studies, such as the Enhancing Neuro Imaging Genetics through Meta-Analysis (ENIGMA) consortium and the IMAGEN study, have suggested that structural brain alterations were heritable and polygenic (Hibar et al., 2015; Stein et al., 2012), and a growing body of evidence has shown the relationship between DNA methylation and brain structural changes in MDD (Wheater et al., 2020). Thus, in the present study, we presumed that among the 2018 DMPs involved in MDD pathophysiology, only a subset might be involved in the depression-related intermediate neuroimaging phenotype. This may explain why several CpG sites related to the diagnosis of MDD were associated with changes in cortical thickness in the present study.

This study had several strengths and limitations. First, we examined the DNA obtained from peripheral blood, which does not directly represent the methylation landscape in the brain tissue. However, previous studies have suggested a concordance between DNA methylation patterns in peripheral lymphocytes and several brain regions (Davies et al., 2012; Horvath et al., 2012). Second, causal relationship between the onset of MDD and DNA methylation level cannot be established in a case-control study and confounding factors should be considered. Although we adjusted DNA methylation results using two confounders (age, sex) and two principal components, there are still potential confounders such as functional polymorphisms and environmental factors (e.g. BMI, smoking, alcohol consumption, physical activity, and other lifestyle factors) that may affect the interpretation of our results. Therefore, our findings should be interpreted with caution and need further validation using

https://doi.org/10.1017/S0033291724000709 Published online by Cambridge University Press

external cohort data. Furthermore, within 10 kb genomic regions centered on each of the 8 CpG sites, we did not observe any significant co-methylation (rho > |0.5|) (online Supplementary Fig. S5). Since the potential impact of multiple CpG sites on cortical thickness might not be fully addressed, further efforts to validate co-methylation using whole-genome bisulfite sequencing are needed. Additionally, the lack of replication and relatively small sample size may limit the reliability of the present study. However, to maximize the statistical power, all samples were included in the discovery group without creating an independent replication group. Although our study is still underpowered in cases where DNA methylation differences are marginal, we comprehensively investigated the potential correlation between epigenetic loci and brain structure (i.e. cortical thickness) in patients with MDD, thereby providing a foundation for translational research in neuroimaging genomics. Future studies with larger sample sizes are expected to support the findings of this study. Finally, we did not provide further validation results at the gene expression level because of the limited sample size in the Gene Expression Omnibus (GEO) database (GSE42546, GSE80655, GSE101521, GSE102556, and GSE185855) (data not shown). Further investigation of our findings, through the combination of epigenomic, genomic, transcriptomic, and metabolomic data, will provide a deeper understanding of the pathophysiological mechanisms underlying MDD.

In conclusion, we found that the cortical thickness of the left VLPFC was negatively correlated with the DNA methylation levels of CpG sites associated with *EML6*, *ZFP64*, *CLSTN3*, *KCNMA1*, *TAOK2*, and *NT5E*, which may affect alterations in brain function and structure. In addition, genes associated with DMPs were enriched in the gene networks involved in CNS morphology and neurodevelopmental disorders. Our findings provide deeper insight into the pathophysiological mechanisms of MDD.

Supplementary material. The supplementary material for this article can be found at https://doi.org/10.1017/S0033291724000709.

Acknowledgements. The authors are grateful to all the participants who volunteered, interviewers, and technicians included in this study. All the authors agree with the published version of the manuscript.

Funding statement. This work was supported by National Research Foundation of Korea (NRF) grants funded by the Korean government (MSIT) (Nos. 2022R1A2C4001313, 2020R1C1C1012288, 2020M3E5D9080792, and 2022R1A2C2093009).

Competing interests. The authors have no potential or actual conflicts of interest.

Ethical standards. The authors assert that all procedures contributing to this work complied with the ethical standards of the relevant national and institutional committees on human experimentation and the Declaration of Helsinki of 1975, as revised in 2008. This study was approved by the Institutional Review Board of Korea University Anam Hospital (protocol code: 2017AN0185 and date of approval: June 5, 2017).

References

Aberg, K. A., Dean, B., Shabalin, A. A., Chan, R. F., Han, L. K. M., Zhao, M., … van den Oord, E. (2020). Methylome-wide association findings for major depressive disorder overlap in blood and brain and replicate in independent brain samples. *Molecular Psychiatry*, *25*(6), 1344–1354. doi:10.1038/s41380-018-0247-6

Ables, J. L., Breunig, J. J., Eisch, A. J., & Rakic, P. (2011). Not(ch) just development: Notch signalling in the adult brain. *Nature Reviews Neuroscience*, *12*(5), 269–283. doi:10.1038/nrn3024

Ambalavanan, A., Girard, S. L., Ahn, K., Zhou, S., Dionne-Laporte, A., Spiegelman, D., … Rouleau, G. A. (2016). De novo variants in sporadic cases of childhood onset schizophrenia. *European Journal of Human Genetics*, *24*(6), 944–948. doi:10.1038/ejhg.2015.218

Bardai, F. H., & D'Mello, S. R. (2011). Selective toxicity by HDAC3 in neurons: Regulation by Akt and GSK3beta. *Journal of Neuroscience*, *31*(5), 1746–1751. doi:10.1523/JNEUROSCI.5704-10.2011

Barnes, J., Mondelli, V., & Pariante, C. M. (2017). Genetic contributions of inflammation to depression. *Neuropsychopharmacology*, *42*(1), 81–98. doi:10.1038/npp.2016.169

Bédard, A., Tremblay, P., Chernomoretz, A., & Vallières, L. (2007). Identification of genes preferentially expressed by microglia and upregulated during cuprizone-induced inflammation. *Glia*, *55*(8), 777–789. doi:10.1002/glia.20477

Bigdeli, T. B., Maher, B. S., Zhao, Z., Sun, J., Medeiros, H., Akula, N., … Fanous, A. H. (2013). Association study of 83 candidate genes for bipolar disorder in chromosome 6q selected using an evidence-based prioritization algorithm. *American Journal of Medical Genetics Part B: Neuropsychiatric Genetics*, *162b*(8), 898–906. doi:10.1002/ajmg.b.32200

Cattarinussi, G., Delvecchio, G., Sambataro, F., & Brambilla, P. (2022). The effect of polygenic risk scores for major depressive disorder, bipolar disorder and schizophrenia on morphological brain measures: A systematic review of the evidence. *Journal of Affective Disorders*, *310*, 213–222. doi:10.1016/j.jad.2022.05.007

Chapman, N. H., Nato, A. Q., Bernier, R., Ankenman, K., Sohi, H., Munson, J., … Wijsman, E. M. (2015). Whole exome sequencing in extended families with autism spectrum disorder implicates four candidate genes. *Human Genetics*, *134*(10), 1055–1068. doi:10.1007/s00439-015-1585-y

Cheng, P., Qiu, Z., & Du, Y. (2021). Potassium channels and autism spectrum disorder: An overview. *International Journal of Developmental Neuroscience*, *81*(6), 479–491. doi:10.1002/jdn.10123

Chiarella, J., Schumann, L., Pomares, F. B., Frodl, T., Tozzi, L., Nemoda, Z., … Booij, L. (2020). DNA methylation differences in stress-related genes, functional connectivity and gray matter volume in depressed and healthy adolescents. *Journal of Affective Disorders*, *271*, 160–168. doi:10.1016/j.jad.2020.03.062

Choi, H.-K., Choi, Y., Kang, H., Lim, E.-J., Park, S.-Y., Lee, H.-S., … Yoon, H.-G. (2015). PINK1 positively regulates HDAC3 to suppress dopaminergic neuronal cell death. *Human Molecular Genetics*, *24*(4), 1127–1141. doi:10.1093/hmg/ddu526

Cukkemane, A., Becker, N., Zielinski, M., Frieg, B., Lakomek, N. A., Heise, H., … Weiergräber, O. H. (2021). Conformational heterogeneity coupled with β-fibril formation of a scaffold protein involved in chronic mental illnesses. *Translational Psychiatry*, *11*(1), 639. doi:10.1038/s41398-021-01765-1

Cunha, R. A. (2016). How does adenosine control neuronal dysfunction and neurodegeneration? *Journal of Neurochemistry*, *139*(6), 1019–1055. doi:10.1111/jnc.13724

Dale, A. M., Fischl, B., & Sereno, M. I. (1999). Cortical surface-based analysis. I. Segmentation and surface reconstruction. *Neuroimage*, *9*(2), 179–194. doi:10.1006/nimg.1998.0395

Datta, D., Arion, D., Corradi, J. P., & Lewis, D. A. (2015). Altered expression of CDC42 signaling pathway components in cortical layer 3 pyramidal cells in schizophrenia. *Biological Psychiatry*, *78*(11), 775–785. doi:10.1016/j.biopsych.2015.03.030

Davies, M. N., Volta, M., Pidsley, R., Lunnon, K., Dixit, A., Lovestone, S., … Mill, J. (2012). Functional annotation of the human brain methylome identifies tissue-specific epigenetic variation across brain and blood. *Genome Biology*, *13*(6), R43. doi:10.1186/gb-2012-13-6-r43

de Baumont, A., Maschietto, M., Lima, L., Carraro, D. M., Olivieri, E. H., Fiorini, A., … Brentani, H. (2015). Innate immune response is differentially dysregulated between bipolar disease and schizophrenia. *Schizophrenia Research*, *161*(2–3), 215–221. doi:10.1016/j.schres.2014.10.055

Destrieux, C., Fischl, B., Dale, A., & Halgren, E. (2010). Automatic parcellation of human cortical gyri and sulci using standard anatomical nomenclature. *Neuroimage*, *53*(1), 1–15. doi:10.1016/j.neuroimage.2010.06.010

https://doi.org/10.1017/S0033291724000709 Published online by Cambridge University Press

Dresselhaus, E. C., & Meffert, M. K. (2019). Cellular specificity of NF-κB function in the nervous system. *Frontiers in Immunology*, *10*, 1043. doi:10.3389/fimmu.2019.01043

Duman, R. S., Aghajanian, G. K., Sanacora, G., & Krystal, J. H. (2016). Synaptic plasticity and depression: New insights from stress and rapid-acting antidepressants. *Nature Medicine*, *22*(3), 238–249. doi:10.1038/nm.4050

Efstathopoulos, P., Andersson, F., Melas, P. A., Yang, L. L., Villaescusa, J. C., Rüegg, J., … Lavebratt, C. (2018). NR3C1 Hypermethylation in depressed and bullied adolescents. *Translational Psychiatry*, *8*(1), 121. doi:10.1038/s41398-018-0169-8

Ferrer, A., Labad, J., Salvat-Pujol, N., Barrachina, M., Costas, J., Urretavizcaya, M., … Soria, V. (2019). BDNF genetic variants and methylation: Effects on cognition in major depressive disorder. *Translational Psychiatry*, *9*(1), 265. doi:10.1038/s41398-019-0601-8

First, M. B., Williams, J. B. W., Karg, R. S., & Spitzer, R. L. (2016). *SCID-5-CV: Structured clinical interview for DSM-5 disorders: Clinician version*. Arlington, VA: American Psychiatric Association Publishing.

Fischl, B., Liu, A., & Dale, A. M. (2001). Automated manifold surgery: Constructing geometrically accurate and topologically correct models of the human cerebral cortex. *IEEE Transactions on Medical Imaging*, *20*(1), 70–80. doi:10.1109/42.906426

Fischl, B., Salat, D. H., Busa, E., Albert, M., Dieterich, M., Haselgrove, C., … Dale, A. M. (2002). Whole brain segmentation: Automated labeling of neuroanatomical structures in the human brain. *Neuron*, *33*(3), 341–355. doi:10.1016/s0896-6273(02)00569-x

Fischl, B., Sereno, M. I., & Dale, A. M. (1999). Cortical surface-based analysis. II: Inflation, flattening, and a surface-based coordinate system. *Neuroimage*, *9*(2), 195–207. doi:10.1006/nimg.1998.0396

Fischl, B., van der Kouwe, A., Destrieux, C., Halgren, E., Ségonne, F., Salat, D. H., … Dale, A. M. (2004). Automatically parcellating the human cerebral cortex. *Cerebral Cortex*, *14*(1), 11–22. doi:10.1093/cercor/bhg087

Flint, J., & Kendler, K. S. (2014). The genetics of major depression. *Neuron*, *81*(3), 484–503. doi:10.1016/j.neuron.2014.01.027

Freytag, V., Carrillo-Roa, T., Milnik, A., Sämann, P. G., Vukojevic, V., Coynel, D., … Papassotiropoulos, A. (2017). A peripheral epigenetic signature of immune system genes is linked to neocortical thickness and memory. *Nature Communications*, *8*, 15193. doi:10.1038/ncomms15193

Fujisawa, T. X., Nishitani, S., Takiguchi, S., Shimada, K., Smith, A. K., & Tomoda, A. (2019). Oxytocin receptor DNA methylation and alterations of brain volumes in maltreated children. *Neuropsychopharmacology*, *44*(12), 2045–2053. doi:10.1038/s41386-019-0414-8

Gao, T.-T., Wang, Y., Liu, L., Wang, J.-L., Wang, Y.-J., Guan, W., … Jiang, B. (2020). LIMK1/2 in the mPFC plays a role in chronic stress-induced depressive-like effects in mice. *International Journal of Neuropsychopharmacology*, *23*(12), 821–836. doi:10.1093/ijnp/pyaa067

Gibitova, E. A., Dobrynin, P. V., Pomerantseva, E. A., Musatova, E. V., Kostareva, A., Evsyukov, I., … Grigorenko, E. L. (2022). A study of the genomic variations associated with autistic spectrum disorders in a Russian cohort of patients using whole-exome sequencing. *Genes*, *13*(5), 920. doi:10.3390/genes13050920

Glahn, D. C., Curran, J. E., Winkler, A. M., Carless, M. A., Kent, J. W. Jr., Charlesworth, J. C., … Blangero, J. (2012). High dimensional endophenotype ranking in the search for major depression risk genes. *Biological Psychiatry*, *71*(1), 6–14. doi:10.1016/j.biopsych.2011.08.022

Gonzales, E. L., Jeon, S. J., Han, K. M., Yang, S. J., Kim, Y., Remonde, C. G., … Shin, C. Y. (2023). Correlation between immune-related genes and depression-like features in an animal model and in humans. *Brain, Behavior, and Immunity*, *113*, 29–43. doi:10.1016/j.bbi.2023.06.017

Gough, S. C. L., & Simmonds, M. J. (2007). The HLA region and autoimmune disease: Associations and mechanisms of action. *Current Genomics*, *8*(7), 453–465. doi:10.2174/138920207783591690

Graw, S., Henn, R., Thompson, J. A., & Koestler, D. C. (2019). pwrEWAS: A user-friendly tool for comprehensive power estimation for epigenome wide association studies (EWAS). *BMC Bioinformatics*, *20*(1), 218. doi:10.1186/s12859-019-2804-7

Gunnersen, J. M., Kim, M. H., Fuller, S. J., De Silva, M., Britto, J. M., Hammond, V. E., … Tan, S.-S. (2007). Sez-6 proteins affect dendritic arborization patterns and excitability of cortical pyramidal neurons. *Neuron*, *56*(4), 621–639. doi:10.1016/j.neuron.2007.09.018

Hall, L. S., Adams, M. J., Arnau-Soler, A., Clarke, T.-K., Howard, D. M., Zeng, Y., … McIntosh, A. M. (2018). Genome-wide meta-analyses of stratified depression in Generation Scotland and UK Biobank. *Translational Psychiatry*, *8*(1), 1–12. doi:10.1038/s41398-017-0034-1

Hamilton, M. (1960). A rating scale for depression. *Journal of Neurology, Neurosurgery, and Psychiatry*, *23*(1), 56–62.

Han, K. M., Choi, K. W., Kim, A., Kang, W., Kang, Y., Tae, W. S., … Ham, B. J. (2022). Association of DNA methylation of the NLRP3 gene with changes in cortical thickness in major depressive disorder. *International Journal of Molecular Sciences*, *23*(10), 5768. doi:10.3390/ijms23105768

Han, K. M., & Ham, B. J. (2021). How inflammation affects the brain in depression: A review of functional and structural MRI studies. *Journal of Clinical Neurology*, *17*(4), 503–515. doi:10.3988/jcn.2021.17.4.503

Han, K. M., Han, M. R., Kim, A., Kang, W., Kang, Y., Kang, J., … Ham, B. J. (2020a). A study combining whole-exome sequencing and structural neuroimaging analysis for major depressive disorder. *Journal of Affective Disorders*, *262*, 31–39. doi:10.1016/j.jad.2019.10.039

Han, K. M., Tae, W. S., Kim, A., Kang, Y., Kang, W., Kang, J., … Ham, B. J. (2020b). Serum FAM19A5 levels: A novel biomarker for neuroinflammation and neurodegeneration in major depressive disorder. *Brain, Behavior, and Immunity*, *87*, 852–859. doi:10.1016/j.bbi.2020.03.021

Hibar, D. P., Stein, J. L., Renteria, M. E., Arias-Vasquez, A., Desrivières, S., Jahanshad, N., … Medland, S. E. (2015). Common genetic variants influence human subcortical brain structures. *Nature*, *520*(7546), 224–229. doi:10.1038/nature14101

Hill, W. D., Marioni, R. E., Maghzian, O., Ritchie, S. J., Hagenaars, S. P., McIntosh, A. M., … Deary, I. J. (2019). A combined analysis of genetically correlated traits identifies 187 loci and a role for neurogenesis and myelination in intelligence. *Molecular Psychiatry*, *24*(2), 169–181. doi:10.1038/s41380-017-0001-5

Hogstrom, L. J., Westlye, L. T., Walhovd, K. B., & Fjell, A. M. (2013). The structure of the cerebral cortex across adult life: Age-related patterns of surface area, thickness, and gyrification. *Cerebral Cortex*, *23*(11), 2521–2530. doi:10.1093/cercor/bhs231

Horvath, S., Zhang, Y., Langfelder, P., Kahn, R. S., Boks, M. P. M., van Eijk, K., … Ophoff, R. A. (2012). Aging effects on DNA methylation modules in human brain and blood tissue. *Genome Biology*, *13*(10), R97. doi:10.1186/gb-2012-13-10-r97

Hoseth, E. Z., Krull, F., Dieset, I., Mørch, R. H., Hope, S., Gardsjord, E. S., … Ueland, T. (2018). Attenuated Notch signaling in schizophrenia and bipolar disorder. *Scientific Reports*, *8*(1), 5349. doi:10.1038/s41598-018-23703-w

Howes, O. D., & Onwordi, E. C. (2023). The synaptic hypothesis of schizophrenia version III: A master mechanism. *Molecular Psychiatry*, *28*(5), 1843–1856. doi:10.1038/s41380-023-02043-w

Hu, H. T., Huang, T. N., & Hsueh, Y. P. (2020). KLHL17/Actinfilin, a brain-specific gene associated with infantile spasms and autism, regulates dendritic spine enlargement. *Journal of Biomedical Science*, *27*(1), 103. doi:10.1186/s12929-020-00696-1

Huang, Y. S., Fang, T. H., Kung, B., & Chen, C. H. (2022). Two genetic mechanisms in Two siblings with intellectual disability, autism spectrum disorder, and psychosis. *Journal of Personalized Medicine*, *12*(6), 1013. doi:10.3390/jpm12061013

Humphreys, K. L., Moore, S. R., Davis, E. G., MacIsaac, J. L., Lin, D. T. S., Kobor, M. S., & Gotlib, I. H. (2019). DNA methylation of HPA-axis genes and the onset of major depressive disorder in adolescent girls: A prospective analysis. *Translational Psychiatry*, *9*(1), 245. doi:10.1038/s41398-019-0582-7

Ignatov, A., Lintzel, J., Hermans-Borgmeyer, I., Kreienkamp, H.-J., Joost, P., Thomsen, S., … Schaller, H. C. (2003). Role of the G-protein-coupled receptor GPR12 as high-affinity receptor for sphingosylphosphorylcholine and its expression and function in brain development. *Journal of Neuroscience*, *23*(3), 907–914. doi:10.1523/JNEUROSCI.23-03-00907.2003

Januar, V., Ancelin, M. L., Ritchie, K., Saffery, R., & Ryan, J. (2015). BDNF promoter methylation and genetic variation in late-life depression. *Translational Psychiatry*, *5*(8), e619. doi:10.1038/tp.2015.114

Johnson, W. E., Li, C., & Rabinovic, A. (2007). Adjusting batch effects in microarray expression data using empirical Bayes methods. *Biostatistics (Oxford, England)*, *8*(1), 118–127. doi:10.1093/biostatistics/kxj037

https://doi.org/10.1017/S0033291724000709 Published online by Cambridge University Press

Kajiwara, Y., McKenzie, A., Dorr, N., Gama Sosa, M. A., Elder, G., Schmeidler, J., … Buxbaum, J. D. (2016). The human-specific CASP4 gene product contributes to Alzheimer-related synaptic and behavioural deficits. *Human Molecular Genetics*, *25*(19), 4315–4327. doi:10.1093/hmg/ddw265

Kajiwara, Y., Schiff, T., Voloudakis, G., Gama Sosa, M. A., Elder, G., Bozdagi, O., & Buxbaum, J. D. (2014). A critical role for human caspase-4 in endotoxin sensitivity. *The Journal of Immunology*, *193*(1), 335–343. doi:10.4049/jimmunol.1303424

Kang, H. J., Kim, J. M., Stewart, R., Kim, S. Y., Bae, K. Y., Kim, S. W., … Yoon, J. S. (2013). Association of SLC6A4 methylation with early adversity, characteristics and outcomes in depression. *Progress in Neuro-Psychopharmacology and Biological Psychiatry*, *44*, 23–28. doi:10.1016/j.pnpbp.2013.01.006

Kang, H. J., Kim, K. T., Yoo, K. H., Park, Y., Kim, J. W., Kim, S. W., … Kim, J. M. (2020). Genetic markers for later remission in response to early improvement of antidepressants. *International Journal of Molecular Sciences*, *21*(14), 4884. doi:10.3390/ijms21144884

Kang, M., Ang, T. F. A., Devine, S. A., Sherva, R., Mukherjee, S., Trittschuh, E. H., … Farrer, L. A. (2023). A genome-wide search for pleiotropy in more than 100000 harmonized longitudinal cognitive domain scores. *Molecular Neurodegeneration*, *18*(1), 40. doi:10.1186/s13024-023-00633-4

Kaufman, J., Wymbs, N. F., Montalvo-Ortiz, J. L., Orr, C., Albaugh, M. D., Althoff, R., … Hudziak, J. (2018). Methylation in OTX2 and related genes, maltreatment, and depression in children. *Neuropsychopharmacology*, *43*(11), 2204–2211. doi:10.1038/s41386-018-0157-y

Kaur, A., Lee, L.-H., Chow, S.-C., & Fang, C.-M. (2018). IRF5-mediated Immune responses and its implications in immunological disorders. *International Reviews of Immunology*, *37*(5), 229–248. doi:10.1080/08830185.2018.1469629

Kessler, R. C., Angermeyer, M., Anthony, J. C., Deg, R., Demyttenaere, K., Gasquet, I., … Ustün, T. B. (2007). Lifetime prevalence and age-of-onset distributions of mental disorders in the world health organization's world mental health survey initiative. *World Psychiatry*, *6*(3), 168–176.

Kim, Y. K., Ham, B. J., & Han, K. M. (2019). Interactive effects of genetic polymorphisms and childhood adversity on brain morphologic changes in depression. *Progress in Neuro-Psychopharmacology and Biological Psychiatry*, *91*, 4–13. doi:10.1016/j.pnpbp.2018.03.009

Klengel, T., & Binder, E. B. (2013). Gene–environment interactions in major depressive disorder. *The Canadian Journal of Psychiatry*, *58*(2), 76–83. doi:10.1177/070674371305800203

Klinger-König, J., Hertel, J., Van der Auwera, S., Frenzel, S., Pfeiffer, L., Waldenberger, M., … Grabe, H. J. (2019). Methylation of the FKBP5 gene in association with FKBP5 genotypes, childhood maltreatment and depression. *Neuropsychopharmacology*, *44*(5), 930–938. doi:10.1038/s41386-019-0319-6

Kupfer, D. J., Frank, E., & Phillips, M. L. (2012). Major depressive disorder: New clinical, neurobiological, and treatment perspectives. *Lancet (London, England)*, *379*(9820), 1045–1055. doi:10.1016/s0140-6736(11)60602-8

Lapato, D. M., Roberson-Nay, R., Kirkpatrick, R. M., Webb, B. T., York, T. P., & Kinser, P. A. (2019). DNA methylation associated with postpartum depressive symptoms overlaps findings from a genome-wide association meta-analysis of depression. *Clinical Epigenetics*, *11*(1), 169. doi:10.1186/s13148-019-0769-z

Laumonnier, F., Roger, S., Guérin, P., Molinari, F., M'Rad, R., Cahard, D., … Briault, S. (2006). Association of a functional deficit of the BKCa channel, a synaptic regulator of neuronal excitability, with autism and mental retardation. *American Journal of Psychiatry*, *163*(9), 1622–1629. doi:10.1176/ajp.2006.163.9.1622

Laurent, L., Wong, E., Li, G., Huynh, T., Tsirigos, A., Ong, C. T., … Wei, C.-L. (2010). Dynamic changes in the human methylome during differentiation. *Genome Research*, *20*(3), 320–331. doi:10.1101/gr.101907.109

Lee, J. J., Wedow, R., Okbay, A., Kong, E., Maghzian, O., Zacher, M., … Cesarini, D. (2018). Gene discovery and polygenic prediction from a genome-wide association study of educational attainment in 1.1 million individuals. *Nature Genetics*, *50*(8), 1112–1121. doi:10.1038/s41588-018-0147-3

Lennon, P. F., Taylor, C. T., Stahl, G. L., & Colgan, S. P. (1998). Neutrophil-derived 5′-adenosine monophosphate promotes endothelial barrier function via CD73-mediated conversion to adenosine and endothelial A2B receptor activation. *The Journal of Experimental Medicine*, *188*(8), 1433–1443.

Li, M., Li, Y., Qin, H., Tubbs, J. D., Li, M., Qiao, C., … Yao, Y. (2021). Genome-wide DNA methylation analysis of peripheral blood cells derived from patients with first-episode schizophrenia in the Chinese Han population. *Molecular Psychiatry*, *26*(8), 4475–4485. doi:10.1038/s41380-020-00968-0

Li, Q. S., Morrison, R. L., Turecki, G., & Drevets, W. C. (2022). Meta-analysis of epigenome-wide association studies of major depressive disorder. *Scientific Reports*, *12*(1), 18361. doi:10.1038/s41598-022-22744-6

Liu, Y.-J., Chen, J., Li, X., Zhou, X., Hu, Y.-M., Chu, S.-F., … Chen, N.-H. (2019). Research progress on adenosine in central nervous system diseases. *CNS Neuroscience & Therapeutics*, *25*(9), 899–910. doi:10.1111/cns.13190

Lopizzo, N., Bocchio Chiavetto, L., Cattane, N., Plazzotta, G., Tarazi, F. I., Pariante, C. M., … Cattaneo, A. (2015). Gene-environment interaction in major depression: Focus on experience-dependent biological systems. *Frontiers in Psychiatry*, *6*, 68. doi:10.3389/fpsyt.2015.00068

Mahady, L., Nadeem, M., Malek-Ahmadi, M., Chen, K., Perez, S. E., & Mufson, E. J. (2018). Frontal cortex epigenetic dysregulation during the progression of Alzheimer's disease. *Journal of Alzheimer's Disease*, *62*(1), 115–131. doi:10.3233/JAD-171032

Malhi, G. S., & Mann, J. J. (2018). Depression. *Lancet (London, England)*, *392*(10161), 2299–2312. doi:10.1016/s0140-6736(18)31948-2

Martin, T. C., Yet, I., Tsai, P. C., & Bell, J. T. (2015). coMET: Visualisation of regional epigenome-wide association scan results and DNA co-methylation patterns. *BMC Bioinformatics*, *16*(1), 131. doi:10.1186/s12859-015-0568-2

Miles, A. E., Dos Santos, F. C., Byrne, E. M., Renteria, M. E., McIntosh, A. M., Adams, M. J., … Nikolova, Y. S. (2021). Transcriptome-based polygenic score links depression-related corticolimbic gene expression changes to sex-specific brain morphology and depression risk. *Neuropsychopharmacology*, *46*(13), 2304–2311. doi:10.1038/s41386-021-01189-x

Nagel, M., Jansen, P. R., Stringer, S., Watanabe, K., de Leeuw, C. A., Bryois, J., … Posthuma, D. (2018). Meta-analysis of genome-wide association studies for neuroticism in 449484 individuals identifies novel genetic loci and pathways. *Nature Genetics*, *50*(7), 920–927. doi:10.1038/s41588-018-0151-7

Nordlund, J., Bäcklin, C. L., Wahlberg, P., Busche, S., Berglund, E. C., Eloranta, M.-L., … Syvänen, A.-C. (2013). Genome-wide signatures of differential DNA methylation in pediatric acute lymphoblastic leukemia. *Genome Biology*, *14*(9), r105. doi:10.1186/gb-2013-14-9-r105

Oldfield, R. C. (1971). The assessment and analysis of handedness: The Edinburgh inventory. *Neuropsychologia*, *9*(1), 97–113. doi:10.1016/0028-3932(71)90067-4

Olshen, A. B., Venkatraman, E. S., Lucito, R., & Wigler, M. (2004). Circular binary segmentation for the analysis of array-based DNA copy number data. *Biostatistics (Oxford, England)*, *5*(4), 557–572. doi:10.1093/biostatistics/kxh008

Osimo, E. F., Pillinger, T., Rodriguez, I. M., Khandaker, G. M., Pariante, C. M., & Howes, O. D. (2020). Inflammatory markers in depression: A meta-analysis of mean differences and variability in 5166 patients and 5083 controls. *Brain, Behavior, and Immunity*, *87*, 901–909. doi:10.1016/j.bbi.2020.02.010

Panizzon, M. S., Fennema-Notestine, C., Eyler, L. T., Jernigan, T. L., Prom-Wormley, E., Neale, M., … Kremen, W. S. (2009). Distinct genetic influences on cortical surface area and cortical thickness. *Cerebral Cortex*, *19*(11), 2728–2735. doi:10.1093/cercor/bhp026

Park, S.-Y., & Kim, J.-S. (2020). A short guide to histone deacetylases including recent progress on class II enzymes. *Experimental & Molecular Medicine*, *52*(2), 204–212. doi:10.1038/s12276-020-0382-4

Penner-Goeke, S., & Binder, E. B. (2019). Epigenetics and depression. *Dialogues in Clinical Neuroscience*, *21*(4), 397–405. doi:10.31887/DCNS.2019.21.4/ebinder

Phillips, M. L., Chase, H. W., Sheline, Y. I., Etkin, A., Almeida, J. R., Deckersbach, T., & Trivedi, M. H. (2015). Identifying predictors, moderators, and mediators of antidepressant response in major depressive disorder: Neuroimaging approaches. *American Journal of Psychiatry*, *172*(2), 124–138. doi:10.1176/appi.ajp.2014.14010076

Pierce, A. M., & Keating, A. K. (2014). TAM Receptor tyrosine kinases: Expression, disease and oncogenesis in the central nervous system. *Brain Research*, *1542*, 206. doi:10.1016/j.brainres.2013.10.049

https://doi.org/10.1017/S0033291724000709 Published online by Cambridge University Press

Puvogel, S., Alsema, A., Kracht, L., Webster, M. J., Weickert, C. S., Sommer, I. E. C., & Eggen, B. J. L. (2022). Single-nucleus RNA sequencing of midbrain blood-brain barrier cells in schizophrenia reveals subtle transcriptional changes with overall preservation of cellular proportions and phenotypes. *Molecular Psychiatry*, *27*(11), 4731–4740. doi:10.1038/s41380-022-01796-0

Richter, M., Murtaza, N., Scharrenberg, R., White, S. H., Johanns, O., Walker, S., … Calderon de Anda, F. (2019). Altered TAOK2 activity causes autism-related neurodevelopmental and cognitive abnormalities through RhoA signaling. *Molecular Psychiatry*, *24*(9), 1329–1350. doi:10.1038/s41380-018-0025-5

Rijlaarsdam, J., Cosin-Tomas, M., Schellhas, L., Abrishamcar, S., Malmberg, A., Neumann, A., … Cecil, C. A. M. (2023). DNA methylation and general psychopathology in childhood: An epigenome-wide meta-analysis from the PACE consortium. *Molecular Psychiatry*, *28*(3), 1128–1136. doi:10.1038/s41380-022-01871-6

Ritchie, M. E., Phipson, B., Wu, D., Hu, Y., Law, C. W., Shi, W., & Smyth, G. K. (2015). Limma powers differential expression analyses for RNA-sequencing and microarray studies. *Nucleic Acids Research*, *43*(7), e47. doi:10.1093/nar/gkv007

Rive, M. M., van Rooijen, G., Veltman, D. J., Phillips, M. L., Schene, A. H., & Ruhé, H. G. (2013). Neural correlates of dysfunctional emotion regulation in major depressive disorder. A systematic review of neuroimaging studies. *Neuroscience & Biobehavioral Reviews*, *37*(10 Pt 2), 2529–2553. doi:10.1016/j.neubiorev.2013.07.018

Rutten, B. P. F., Vermetten, E., Vinkers, C. H., Ursini, G., Daskalakis, N. P., Pishva, E., … Boks, M. P. M. (2018). Longitudinal analyses of the DNA methylome in deployed military servicemen identify susceptibility loci for post-traumatic stress disorder. *Molecular Psychiatry*, *23*(5), 1145–1156. doi:10.1038/mp.2017.120

Sakamoto, K., Tamamura, Y., Katsube, K., & Yamaguchi, A. (2008). Zfp64 participates in Notch signaling and regulates differentiation in mesenchymal cells. *Journal of Cell Science*, *121*(Pt 10), 1613–1623. doi:10.1242/jcs.023119

Saxonov, S., Berg, P., & Brutlag, D. L. (2006). A genome-wide analysis of CpG dinucleotides in the human genome distinguishes two distinct classes of promoters. *Proceedings of the National Academy of Sciences*, *103*(5), 1412–1417. doi:10.1073/pnas.0510310103

Schmaal, L., Hibar, D. P., Sämann, P. G., Hall, G. B., Baune, B. T., Jahanshad, N., … Veltman, D. J. (2017). Cortical abnormalities in adults and adolescents with major depression based on brain scans from 20 cohorts worldwide in the ENIGMA Major Depressive Disorder Working Group. *Molecular Psychiatry*, *22*(6), 900–909. doi:10.1038/mp.2016.60

Schneider, I., Kugel, H., Redlich, R., Grotegerd, D., Bürger, C., Bürkner, P. C., … Hohoff, C. (2018). Association of serotonin transporter gene AluJb methylation with major depression, amygdala responsiveness, 5-HTTLPR/rs25531 polymorphism, and stress. *Neuropsychopharmacology*, *43*(6), 1308–1316. doi:10.1038/npp.2017.273

Ségonne, F., Pacheco, J., & Fischl, B. (2007). Geometrically accurate topology-correction of cortical surfaces using nonseparating loops. *IEEE Transactions on Medical Imaging*, *26*(4), 518–529. doi:10.1109/tmi.2006.887364

Shaw, C. A., Li, Y., Wiszniewska, J., Chasse, S., Zaidi, S. N. Y., Jin, W., … Szigeti, K. (2011). Olfactory copy number association with age at onset of Alzheimer disease. *Neurology*, *76*(15), 1302–1309. doi:10.1212/WNL.0b013e3182166df5

Sherva, R., Zhang, R., Sahelijo, N., Jun, G., Anglin, T., Chanfreau, C., … Logue, M. W. (2023). African ancestry GWAS of dementia in a large military cohort identifies significant risk loci. *Molecular Psychiatry*, *28*(3), 1293–1302. doi:10.1038/s41380-022-01890-3

Shinde, V., Sobreira, N., Wohler, E. S., Maiti, G., Hu, N., Silvestri, G., … Chakravarti, S. (2021). Pathogenic alleles in microtubule, secretory granule and extracellular matrix-related genes in familial keratoconus. *Human Molecular Genetics*, *30*(8), 658–671. doi:10.1093/hmg/ddab075

Stein, J. L., Medland, S. E., Vasquez, A. A., Hibar, D. P., Senstad, R. E., Winkler, A. M., … Thompson, P. M. (2012). Identification of common variants associated with human hippocampal and intracranial volumes. *Nature Genetics*, *44*(5), 552–561. doi:10.1038/ng.2250

Steinberg, S., de Jong, S., Mattheisen, M., Costas, J., Demontis, D., Jamain, S., … Stefansson, K. (2014). Common variant at 16p11.2 conferring risk of psychosis. *Molecular Psychiatry*, *19*(1), 108–114. doi:10.1038/mp.2012.157

Sudarov, A., Zhang, X. J., Braunstein, L., LoCastro, E., Singh, S., Taniguchi, Y., … Ross, M. E. (2018). Mature hippocampal neurons require LIS1 for synaptic integrity: Implications for cognition. *Biological Psychiatry*, *83*(6), 518–529. doi:10.1016/j.biopsych.2017.09.011

Suderman, M., Staley, J. R., French, R., Arathimos, R., Simpkin, A., & Tilling, K. (2018). Dmrff: Identifying differentially methylated regions efficiently with power and control. *BioRxiv*, 508556. doi:10.1101/508556

Suh, J. S., Schneider, M. A., Minuzzi, L., MacQueen, G. M., Strother, S. C., Kennedy, S. H., & Frey, B. N. (2019). Cortical thickness in major depressive disorder: A systematic review and meta-analysis. *Progress in Neuro-Psychopharmacology and Biological Psychiatry*, *88*, 287–302. doi:10.1016/j.pnpbp.2018.08.008

Tabarés-Seisdedos, R., Escámez, T., Martínez-Giménez, J. A., Balanzá, V., Salazar, J., Selva, G., … Martínez, S. (2006). Variations in genes regulating neuronal migration predict reduced prefrontal cognition in schizophrenia and bipolar subjects from Mediterranean Spain: A preliminary study. *Neuroscience*, *139*(4), 1289–1300. doi:10.1016/j.neuroscience.2006.01.054

Teschendorff, A. E., Marabita, F., Lechner, M., Bartlett, T., Tegner, J., Gomez-Cabrero, D., & Beck, S. (2013). A beta-mixture quantile normalization method for correcting probe design bias in illumina infinium 450 k DNA methylation data. *Bioinformatics (Oxford, England)*, *29*(2), 189–196. doi:10.1093/bioinformatics/bts680

Tian, Y., Morris, T. J., Webster, A. P., Yang, Z., Beck, S., Feber, A., & Teschendorff, A. E. (2017). ChAMP: Updated methylation analysis pipeline for Illumina BeadChips. *Bioinformatics (Oxford, England)*, *33*(24), 3982–3984. doi:10.1093/bioinformatics/btx513

Tozzi, L., Farrell, C., Booij, L., Doolin, K., Nemoda, Z., Szyf, M., … Frodl, T. (2018). Epigenetic changes of FKBP5 as a link connecting genetic and environmental risk factors with structural and functional brain changes in major depression. *Neuropsychopharmacology*, *43*(5), 1138–1145. doi:10.1038/npp.2017.290

Troubat, R., Barone, P., Leman, S., Desmidt, T., Cressant, A., Atanasova, B., … Belzung, C. (2021). Neuroinflammation and depression: A review. *European Journal of Neuroscience*, *53*(1), 151–171. doi:10.1111/ejn.14720

Uchida, S., Yamagata, H., Seki, T., & Watanabe, Y. (2018). Epigenetic mechanisms of major depression: Targeting neuronal plasticity. *Psychiatry and Clinical Neurosciences*, *72*(4), 212–227. doi:10.1111/pcn.12621

Um, J. W., Pramanik, G., Ko, J. S., Song, M. Y., Lee, D., Kim, H., … Ko, J. (2014). Calsyntenins function as synaptogenic adhesion molecules in concert with neurexins. *Cell Reports*, *6*(6), 1096–1109. doi:10.1016/j.celrep.2014.02.010

Van der Auwera, S., Peyrot, W. J., Milaneschi, Y., Hertel, J., Baune, B., Breen, G., … Grabe, H. (2018). Genome-wide gene-environment interaction in depression: A systematic evaluation of candidate genes: The childhood trauma working-group of PGC-MDD. *American Journal of Medical Genetics Part B: Neuropsychiatric Genetics*, *177*(1), 40–49. doi:10.1002/ajmg.b.32593

Wheater, E. N. W., Stoye, D. Q., Cox, S. R., Wardlaw, J. M., Drake, A. J., Bastin, M. E., & Boardman, J. P. (2020). DNA methylation and brain structure and function across the life course: A systematic review. *Neuroscience & Biobehavioral Reviews*, *113*, 133–156. doi:10.1016/j.neubiorev.2020.03.007

Winham, S. J., Cuellar-Barboza, A. B., McElroy, S. L., Oliveros, A., Crow, S., Colby, C. L., … Biernacka, J. M. (2014). Bipolar disorder with comorbid binge eating history: A genome-wide association study implicates APOB. *Journal of Affective Disorders*, *165*, 151–158. doi:10.1016/j.jad.2014.04.026

Won, E., Choi, S., Kang, J., Kim, A., Han, K. M., Chang, H. S., … Ham, B. J. (2016). Association between reduced white matter integrity in the corpus callosum and serotonin transporter gene DNA methylation in medication-naive patients with major depressive disorder. *Translational Psychiatry*, *6*(8), e866. doi:10.1038/tp.2016.137

Woodbury-Smith, M., Lamoureux, S., Begum, G., Nassir, N., Akter, H., O'Rielly, D. D., … Uddin, M. (2022). Mutational landscape of autism spectrum disorder brain tissue. *Genes*, *13*(2), 207. doi:10.3390/genes13020207

Wu, H., Li, H., Bai, T., Han, L., Ou, J., Xun, G., … Xia, K. (2020). Phenotype-to-genotype approach reveals head-circumference-associated genes in an autism spectrum disorder cohort. *Clinical Genetics*, *97*(2), 338–346. doi:10.1111/cge.13665

https://doi.org/10.1017/S0033291724000709 Published online by Cambridge University Press

Xu, C., Mullersman, J. E., Wang, L., Bin Su, B., Mao, C., Posada, Y., … Wang, K.-S. (2013). Polymorphisms in seizure 6-like gene are associated with bipolar disorder I: Evidence of gene × gender interaction. *Journal of Affective Disorders*, *145*(1), 95–99. doi:10.1016/j.jad.2012.07.017

Xue, W., Tan, W., Dong, L., Tang, Q., Yang, F., Shi, X., … Qian, Y. (2020). TNFAIP8 influences the motor function in mice after spinal cord injury (SCI) through meditating inflammation dependent on AKT. *Biochemical and Biophysical Research Communications*, *528*(1), 234–241. doi:10.1016/j.bbrc.2020.05.029

Yrondi, A., Fiori, L. M., Nogovitsyn, N., Hassel, S., Théroux, J. F., Aouabed, Z., … Turecki, G. (2021). Association between the expression of lncRNA BASP-AS1 and volume of right hippocampal tail moderated by episode duration in major depressive disorder: A CAN-BIND 1 report. *Translational Psychiatry*, *11*(1), 469. doi:10.1038/s41398-021-01592-4

Zhang, H. F., Mellor, D., & Peng, D. H. (2018). Neuroimaging genomic studies in major depressive disorder: A systematic review. *CNS Neuroscience & Therapeutics*, *24*(11), 1020–1036. doi:10.1111/cns.12829

Zhang, Y., Su, Q., Xia, W., Jia, K., Meng, D., Wang, X., … Su, Z. (2023). MiR-140-3p directly targets Tyro3 to regulate OGD/R-induced neuronal injury through the PI3K/Akt pathway. *Brain Research Bulletin*, *192*, 93–106. doi:10.1016/j.brainresbull.2022.11.007

Zhou, W., Chen, L., Jiang, B., Sun, Y., Li, M., Wu, H., … Qin, S. (2021). Large-scale whole-exome sequencing association study identifies FOXH1 gene and sphingolipid metabolism pathway influencing major depressive disorder. *CNS Neuroscience & Therapeutics*, *27*(11), 1425–1428. doi:10.1111/cns.13733

Zhou, W., Laird, P. W., & Shen, H. (2017). Comprehensive characterization, annotation and innovative use of Infinium DNA methylation BeadChip probes. *Nucleic Acids Research*, *45*(4), e22. doi:10.1093/nar/gkw967

https://doi.org/10.1017/S0033291724000709 Published online by Cambridge University Press